Biomaterials Science

Light-reactive dextran gels with immobilized guidance cues for directed neurite growth in 3D models

SCHOLARONE™
Manuscripts

Light-reactive dextran gels with immobilized guidance cues for directed neurite growth in 3D models

Elaine L. Horn-Ranney, Parastoo Khoshakhlagh, Julie W. Kaiga, Michael J. Moore*
Department of Biomedical Engineering, Tulane University, New Orleans, LA, USA

* Corresponding author: mooremj@tulane.edu

Abstract: We present here a novel light-reactive dextran gel for immobilizing guidance cues in neural growth models. The dextran gel is functionalized with glycidyl methacrylate to afford crosslinking abilities, and is combined with polyethylene glycol (PEG) acrylate grafted with thiol groups caged by a UV-light sensitive moiety. The gel is chemically crosslinked within a cell-restrictive PEG micromold with two channels, then irradiated with UV light to liberate the thiol groups in a spatially defined manner. Maleimide-conjugated NeutrAvidin (NA), neurotrophin-3 (NT-3) and semaphorin 3A (Sema3A) are then bound to the free thiols, resulting in regions of immobilized guidance cues. Dorsal root ganglia explants were cultured in these dual hydrogel constructs, and the neurite response quantified by comparing the neurite growth in the channel with the immobilized cue to the channel without any protein. We found that immobilized NT-3 elicited a moderate attractive response, while bound Sema3A elicited a strong repulsive response from neurites. This work establishes a model for investigating growth cone responses to immobilized cues in three dimensions.

Keywords: Neurotrophin-3, semaphorin 3A, nerve guidance, photolithography, dextran.

1. Introduction

Neural navigation during embryonic development depends on chemotactic and haptotactic cues to synapse neurites with their appropriate targets. Axon growth cones from dorsal root ganglia (DRG) interpret these cues through metabolic pathways associated with specific receptor-ligand interactions, resulting in dynamic responses to changes in the *in vivo* environment [1]. Some of these cues have been characterized and translated to an *in vitro* setting in order to recreate these *in vivo* phenomena in cell culture models for wound healing and disease studies [2, 3].

Chemoattractive cues like nerve growth factor (NGF) and neurotrophin-3 (NT-3) are secreted by target cells to form soluble concentration gradients or immobilized in the extracellular matrix via affinity interactions [4-6]. Both NGF and NT-3 have been utilized in *in vitro* studies to elicit attractive responses from neural cultures. One study fabricated 3D growth models using poly(2-hydroxyethyl-methacrylate) and poly(L-lysine) with immobilized gradients of NGF and NT-3 and observed a graded attractive response by DRG neurites to the immobilized cues [7]. Neurites have also been shown to navigate toward sources of soluble NGF and NT-3 gradients in 2D models for controlled growth [8]. Other studies have focused on the interaction of NT-3 with muscle fibers, as NT-3 plays a supportive role in maintaining proprioceptive axons after they have synapsed with their targets [9-11]. As a wound-healing model, NT-3 delivered to the site of spinal cord injury in rats via NT-3-loaded gels [12] or NT-3-expressing lentiviral vectors [13] significantly improved functional recovery of axons. Though the effectiveness of soluble NT-3 was limited by distance, the NT-3 gradient produced by the vectors was enough to overcome the glial scar at the site of the spinal cord injury. As a chemoattractant for proprioceptive neurites, NT-3 has also been observed to be upregulated at the site of cutaneous nerve injury [14]. Conversely, overexpression of NT-3 has been shown to result in limb proprioceptive deficits in spite of no apparent nerve loss, further supporting the importance of NT-3 as a maintenance factor for neurites [15].

Semaphorin 3A (Sema3A) is a chemorepulsive factor that may be expressed as soluble gradients or immobilized transmembrane proteins that bind to the plexin/neuropilin receptor complex in axons to initiate the depolymerization of actin filaments [16, 17]. This response induces growth cone collapse in the presence of Sema3A, causing the axon to turn away from the source of the repulsive cue. For pyramidal neurons, Sema3A repels axons but acts as a chemoattractant for apical dendrites in order to orient the neurons appropriately [18]. As a repulsive cue, Sema3A prevents neurites from navigating away from their targets, and is essential in the pruning of errant axons during nerve mapping. Two dimensional *in vitro* models have observed strong graded responses by DRG neurites to both immobilized and soluble Sema3A, highlighting the sensitivity of axons to chemorepellant cues [19, 20]. This sensitivity persists in fully developed nervous systems, as Sema3A is an inhibitory cue found at nerve injury sites that severely hampers axon regeneration [21, 22]. To eliminate the effects of Sema3A in spinal cord injury, one study administered a Sema3A inhibitor to adult rats at the lesion site [23]. This inhibitor effectively prevented Sema3A from interacting with regenerating axons and allowed axon navigation through the lesion site.

Light-sensitive gels have been used previously for the immobilization of guidance cues within hydrogel cell culture models to provide spatial control over the location of proteins within a growth substrate. Thiol-based chemistries have been utilized extensively for introducing patterned guidance cues [24-26]. Gels that crosslink in the presence of light can physically entrap proteins within the mesh of the hydrogel network, and some studies have fabricated gels with protein gradients with this method [7, 8]. Another method incorporates photolabile nitrobenzyl-based caging moieties into gels to allow proteins to be covalently bound to the hydrogel matrix in very spatially defined regions after the gel has formed [27-29]. These methods have been utilized in the development of nerve growth models for eliciting physiological responses from *in vitro* cultured neurites.

Nerve growth models have been critical for discovering specific receptor-ligand interactions for directing neurite growth in controlled manners. Our goal is to develop a neurite culture platform that

can present physiological cues in a 3D, *in vitro* setting for investigation of growth cone responses. We have previously utilized a dynamic mask photolithography device to develop 3D dual hydrogel constructs with a cell-permissive agarose gel and a cell-restrictive PEG boundary that incorporated both immobilized and soluble cues [28, 30]. Here we present a photoreactive dextran gel as a cell-permissive substrate for immobilizing guidance cues within a dual hydrogel construct. To this dextran gel, we introduced chemoattractive NT-3 and chemorepulsive Sema3A and observed the response of neurites from DRGs to these cues. Dextran has not yet been explored as a substrate for neural growth, but its ability to be functionalized and limited interfering side groups make it an attractive candidate for nerve growth models. This study demonstrates how 3D presentation of immobilized cues influences growth cone responses in an *in vitro* model.

2.   Methods and Materials

All chemicals were purchased and used as received from Sigma Aldrich unless otherwise noted.

2.1 Synthesis of photoreactive reagents

The photolabile compound S-(α-carboxy-2-nitrobenzyl)-L-cysteine methyl ester (CNBC(OMe)) was synthesized according to the detailed protocol published by Horn-Ranney, et al [28]. The CNBC(OMe) compound was then conjugated to a polyethylene glycol (PEG) spacer. Briefly, 0.1 g acryl-PEG-succinimidyl valerate (A-PEG-SVA, MW = 3400; Laysan Bio, Arab, AL) was dissolved in 1.5 ml dimethyl sulfoxide (DMSO). Next, 4.1 µl triethylamine (1 molar eq to A-PEG-SVA) was added to the solution dropwise. A 3 molar equivalent of CNBC(OMe) to Acryl-PEG-SVA (0.027 g) was dissolved in 0.5 ml DMSO, then added to the Acryl-PEG-SVA solution dropwise. The reaction stirred at room temperature overnight. The solution was then added to a dialysis cassette (MWCO = 2000) and dialyzed in water for 2 d, followed by lyophilization for 3d to yield Acryl-PEG-CNBC(OMe)(>99%; ^{1}H NMR (DMSO-d_6): δ 8.0-7.5

(m, 4H, Ar), δ 6.5 (d, 1H, CH_2), δ 6.2 (m, 1H, CH), δ 6.0 (d, 1H, CH_2), δ 3.5 (t, 3H, OCH_3), δ 3.1-2.9 (m, 2H, CH_2)). The structures of the reagents and product are show in Figure 1.

Glycidyl methacrylate (GMA) was grafted to dextran (MW = 70 kDa) according to a published procedure [31]. First, 0.5 g dextran was dissolved in 4.5 ml DMSO under nitrogen. Next, 0.1 g 4-dimethylaminopyridine was dissolved in 0.5 ml DMSO and added to the reaction dropwise, followed by 116 µl GMA. The solution was degassed with nitrogen for 10 min, then stirred for 48 h at room temperature. The reaction was quenched by adding 140 ul 37% HCl, then dialyzed in water for 3 d. The solution was lyophilized to yield glycidyl methacrylate-dextran (Me-Dex; ^{1}H NMR (D_2O): δ 6.1-5.7 (m, 2H, CH_2), δ 5.2 (m, 1H, CH), δ 4.9 (m, 1H, CH), δ 1.9 (s, 3H, CH_3)). The degree of substitution was determined by adding the integrals from protons of the double bond of the methacrylate group (δ 6.1-5.7 ppm) and dividing this sum by the integral from the anomeric proton of the dextran ring (δ 4.9 ppm). The final value from this calculation was multiplied by 100 to give a 42% degree of substitution of Me-Dex.

2.2 Fabrication of dual hydrogel constructs

A dynamic mask projection photolithography apparatus consisting of a UV light source (OmniCure 1000 with 320-500 nm filter, EXFO, Quebec, Canada) with collimating adapter (EXFO), a DMD as a dynamic photomask (Discovery™ 3000, Texas Instruments, Dallas, TX), and a 2X objective lens (Plan Fluor, Nikon Instruments, Tokyo, Japan) was used for hydrogel patterning, as previously described [28, 30]. The UV light was focused at the surface of the cell culture insert membrane to allow bulk irradiation through the depth of the photoreactive material at an intensity of 181 mW/cm^2.

The dual hydrogel system consisted of a photoreactive dextran (PR-Dex) gel in a PEG mold on a permeable cell culture insert. The walls of collagen-coated, 6-well PTFE cell culture inserts with a diameter of 24 mm and pore size of 0.4 µm (Transwell®, Corning Inc., Corning, NY) were treated with Rain-X (SOPUS Products, Houston, TX) to minimize meniscus formation. A solution of 10% w/v PEG-

diacrylate (MW = 1000; Polysciences Inc., Warrington, PA) and 0.5% Irgacure 2959 (Ciba Specialty

Chemicals, Basel, Switzerland) in water was added to the treated inserts (500 μl per insert), followed by

irradiation with UV light from the photolithography apparatus for 55 s per construct to yield

photocrosslinked PEG molds on the cell culture insert membrane. The PEG molds have two channels to

represent a choice point for neurites. Inserts were washed with PBS to remove uncrosslinked PEG

solution.

The cell-permissive PR-Dex gel was chemically crosslinked using a standard ammonium

persulfate (AP)/tetramethylethylenediamine (TEMED) technique. The acrylate groups from the Acryl-

PEG-CNBC(OMe) integrated with the methacrylate network of Me-Dex to afford photocaged sites for

biomolecule immobilization. Murine laminin-1 (Gibco-Invitrogen, Carlsbad, CA) was added to the PR-

Dex gel solution to provide sites for cell attachment. The gel was prepared by combining 29.4 μl 10%

w/v Me-Dex in water, 9.0 μl 20% w/v Acryl-PEG-CNBC(OMe) in water, 6.0 μl 2M ammonium persulfate,

12.6 μl PBS, 0.3 μl laminin (1 mg/ml) and 3 μl 2M TEMED. The PEG molds were filled with approximately

5 μl of this PR-Dex solution, and the PR-Dex gels were fully formed after 30 min. Between 4 and 6 dual

hydrogel constructs were fabricated on each 6-well cell culture insert. Since all PR-Dex gels tested in this

study contained laminin, the abbreviation "PR-Dex" refers to PR-Dex gels with laminin, henceforth.

2.3 Rheological evaluation of gels

Dynamic mechanical analysis of the PR-Dex gels using an AR2000 rheometer (Texas Instruments)

was performed in order to determine the modulus. An oscillating 1° steel cone applied a constant strain

of 4% across a frequency range of 0.100 to 100 Hz, and the storage (G') and loss (G'') moduli were

obtained. Mean storage moduli of gels were analyzed at 10 Hz by one-way ANOVA.

2.4 Immobilization of proteins in gels

Once the dual hydrogel constructs were complete, specified regions of PR-Dex were irradiated with UV light for 90 sec to liberate the carboxy-nitrobenzyl (CNB) moiety from Acryl-PEG-CNBC(OMe) and subsequently present free thiol groups for biomolecule immobilization. The inserts soaked in 5% w/v bovine serum albumin (BSA) in PBS for 1 h to block non-specific binding. The chemoattractive molecule neurotrophin-3 (NT-3; R&D Systems, Minneapolis, MN) and chemorepulsive molecule semaphorin 3A (Sema3A; R&D Systems) were preconjugated with fluorescent secondary antibodies (Alexa Fluor 488 Goat anti-Human IgG (H+L), AF488-Ab; Jackson Immuno, West Grove, PA) by anti-human IgG affinity with the recombinant human NT-3 and Sema3A. Briefly, 15 µl of 0.5 nM NT-3 and 23 µl of 0.2 nM Sema3A were each mixed with 1 µl of 1 mg/ml AF488-Ab solution (134 nmol antibody/nmol protein), and allowed to react overnight at 4°C. Antibody preconjugation was used for observation and quantification of protein binding, and was not used when neurite outgrowth experiments were performed. To afford reactivity to thiol groups, the proteins were conjugated with a maleimide-containing crosslinker (Sulfosuccinimidyl-4-(N-maleimidomethyl)cyclohexane-1-carboxylate (Sulfo-SMCC; Thermo Scientific, Rockford, IL). To the NT-3 solution, 4 µl of 1 mg/ml Sulfo-SMCC in water was added, and 10 µl Sulfo-SMCC was added to the Sema3A solution for a final molar ratio of 146 nmol Sulfo-SMCC/nmol protein. The reaction was carried out for 15 min at 4°C, the volume of each solution increased to 70 µl by adding water, then filtered over spin columns (MWCO = 7 kDa; Thermo Scientific). Each protein solution was added to 900 µl PBS, then subsequently added to the well of a 6-well plate containing the cell culture inserts. As a control, 1 ml of a 20 nM maleimide-activated NeutrAvidin (NA; Thermo Scientific) in PBS was added to a well with a cell culture insert. The inserts soaked in their respective protein solutions for 48 h at 4°C, then washed thoroughly with 2% w/v BSA in PBS to remove unbound proteins. For the NA-inserts, a 1.5 ml solution of 10 µM Alexa Fluor 488 biocytin salt (AF488-biocytin; Molecular Probes, Eugene, OR) was added to the well after washing out excess NA. The inserts

soaked in the AF488-biocytin overnight at 4°C, then washed thoroughly with 2% w/v BSA in PBS. The

fabrication scheme for preparing dual hydrogel constructs with immobilized proteins is presented in

Figure 2.

Bound proteins were quantified by comparing relative fluorescence to known standards. First,

standard curves of known concentrations AF488-Ab/AF488-biocytin were assembled to measure the

concentration of the fluorescent tag in the dual hydrogel constructs. Then, solutions of known protein

concentration and unknown fluorescent tag concentration were compared against the standard curve to

derive a relationship between protein concentration and the associated fluorescent tag. This

relationship was used to convert the concentration of AF488-Ab/AF488-biocytin to protein

concentration, and subsequently quantify the bound protein in each gel. Because of the

autofluorescence of PR-Dex gels, calculations were normalized by subtracting this background

fluorescence from measured fluorescence values of bound proteins in gels.

2.5 Varying irradiation time and photoreactive reagents in gels

Both irradiation time and the concentration of Acryl-PEG-CNBC(OMe) in PR-Dex were varied in

order to determine their effects on biomolecule immobilization. To investigate how irradiation time

affects biomolecule immobilization, PR-Dex gels were prepared as described in Section 2.2. These gels

were then irradiated with UV light for 10, 30, 60, or 90 seconds. Following irradiation, the gels were

blocked with 5% w/v BSA for one hour. The gels soaked in a solution of 1 μg/ml of maleimide-

conjugated Texas Red (MI-TR; Invitrogen) in PBS overnight at 4°C, then washed thoroughly with 2% w/v

BSA.

To determine the effect of CNBC(OMe) concentration on biomolecule immobilization, PR-Dex

gels were prepared as described in Section 2.2, but with fractions of Acryl-PEG-CNBC(OMe) substituted

with Acryl-PEG-SVA in order to decrease the overall concentration of CNBC(OMe) present in the gels.

Gel s with final concentrations of 8.08, 6.06, 4.04, and 2.02 mM Acryl-PEG-CNBC(OMe) in PR-Dex were prepared, then irradiated with UV light for 90 sec and blocked with 5% w/v BSA. These gels soaked in 1 µg/ml MI-TR in PBS overnight at 4°C, then washed with 2% w/v BSA.

Immobilized MI-TR molecules in all gels were quantified by comparing relative fluorescence of MI-TR in PR-Dex gels to that of a standard curve prepared with known concentrations, as described in Section 2.4.

2.6 Culturing dorsal root ganglia in dual hydrogel constructs

All procedures involving vertebrate animals were approved by the Institutional Animal Care and Use Committee. Inserts prepared with immobilized proteins in dual hydrogel constructs were soaked overnight at 37°C in 1.5 ml adhesion media (Neurobasal medium supplemented with L-glutamine (L-Glu), nerve growth factor (NGF), 10% fetal bovine serum, and penicillin/streptomycin; Invitrogen). Cervical dorsal root ganglia (DRGs) isolated from embryonic day 15 Long-Evans rat pups (Charles River, Wilmington, MA) were inserted into each gel by making a small slit in the gel and gently pushing the DRG explant through the gel using forceps. The explants were maintained in growth medium (Neurobasal medium supplemented with B-27, L-glu, NGF, and penicillin/streptomycin) in an incubator (37°C, 5% CO_2) for 5 d, with media changes every 48 h.

After 5 d, the DRGs were fixed in 4% paraformaldehyde for 2 h at 37°C, then washed with 0.1% w/v saponin in PBS. Neurites were tagged with mouse monoclonal [2G10] neuron-specific βIII tubulin primary antibody (AbCam, Cambridge, MA), followed by fluorescent tagging with Cy 3.5-conjugated goat anti-mouse IgG (H+L) secondary antibody (Jackson Immuno). The glial cell marker S100 was tagged with rabbit polyclonal S100 antibody (AbCam), followed by fluorescent tagging with Alexa Fluor 488-conjugated goat anti-rabbit IgG (H+L) secondary antibody (Jackson Immuno). The staining and tagging steps were carried out in 2% BSA/0.1% saponin in PBS, followed by 0.1% saponin washes. Fluorescent

imaging was carried out using a Nikon AZ100 stereo zoom microscope. Confocal imaging was carried out

using a Nikon A1 confocal laser microscope system. Z-stack projection images were depth-coded to

visualize 3D neurite growth.

2.7 Quantification of neurite response

Fluorescent images were processed with Image J software (National Institutes of Health,

Bethesda, MD). Images were thresholded to produce binary representations of fluorescent-tagged

neurites, in which the pixels comprising of neurites have a value of 1 (black) and non-fluorescent regions

have pixels with a value of 0 (white). Regions of interest (ROI) were analyzed in each channel of the

construct. For the channel with the immobilized protein, the ROI was taken as a trapezoidal shape, with

one side along the immobilized cue boundary, and the remaining 3 sides square with the channel

boundaries. For the channel without immobilized protein, a rectangular ROI was taken. Both ROI had

equal areas of 2.50 mm^2. These ROI of unequal shape and equal area were taken to best represent the

opportunity for neurites to grow in one channel versus the other, such that the area of neurite growth in

either channel was equal without the presence of guidance cues. From these ROI, the area fraction

(non-zero area, %A) was measured. To compare the neurite growth in channels with (%$A_{protein}$) and

without (%$A_{no\ protein}$) immobilized protein, a guidance ratio was calculated to be the difference in area

fractions between the channels divided by the total area fraction [19]:

$$Guidance\ ratio = \frac{\%A_{protein}\ -\ \%A_{no\ protein}}{\%A_{protein}\ +\ \%A_{no\ protein}}$$

This guidance ratio is normalized by the total neurite outgrowth in the individual dual hydrogel

constructs, rendering it independent of total neurite growth across all gels. A positive value for the

guidance ratio indicated a chemoattractive response, while a negative value indicated a repulsive

response. Gels with no neurite growth in either channel, likely due to damage sustained by the DRG

explant during dissection and/or insertion, were excluded from the study. Statistical evaluation of

neurite responses to immobilized proteins was determined by one-way ANOVA, with post-hoc analysis

performed with Tukey method.

3. Results

3.1 Concentration of immobilized guidance cues

The photolithography apparatus allowed for both structural and molecular micropatterning of

light-sensitive gels in a reproducible manner. Both the PEG molds and PR-Dex gels maintained their

structural integrity throughout all fabrication steps. Rheological analysis determined the storage

modulus of PR-Dex to be 91.7 ± 1.09 Pa (n = 3). This magnitude of stiffness is on the low end of the

range typically used for neurite growth (~100 – 1000 Pa) [32], and comparable to 0.15% Puramatrix (~100

Pa) [33], which we had used previously in these neurite growth model systems [30].

Figure 3 shows a representative image of immobilized protein (NA tagged with AF488-biocytin)

in the dual hydrogel constructs. Protein immobilization occurred only in the regions of PR-Dex irradiated

by UV light, and was not present in either PEG or unirradiated sections of PR-Dex. The discrepancy in

brightness between the PEG mold and unirradiated PR-Dex was due to the autofluorescence of the PR-

Dex gel itself. Confocal imaging of the bound NA (Fig. 3) shows homogenous binding of proteins

throughout the depth of the gel (227 µm) with some fluorescent biocytin trapped in the cell culture

insert membrane (bottom plane of image). Because the protein was present in relatively equal

concentration throughout the PR-Dex gel, neurites cultured in the dual hydrogel constructs encountered

the same concentration of protein regardless of the plane on which the neurite extended. Irradiation of

PR-Dex using the photolithography apparatus afforded sharp edges to immobilized protein regions,

demonstrating fine control of the spatial distribution of proteins.

The concentration of immobilized cues was quantified in constructs using standard curves of

relative fluorescence. From Table 1, the concentration of immobilized NA was 122 ± 2.50 nM (n = 6),

immobilized NT-3 was 151 ± 15.7 nM (n = 4), and immobilized Sema3A was 87.6 ± 6.74 nM (n = 4). The

immobilization of proteins was consistent across constructs with the same protein. The molecular

weights for these are also listed in Table 1, with NT-3 having a low molecular weight (13.6 kDa), NA

having a medium molecular weight (60.0 kDa), and Sema3A having a high molecular weight (114 kDa).

Though the molecular weights of these proteins vary widely, they bound to the gel in similar quantities,

indicating that the concentration of CNBC in the PR-Dex gel is a more important factor than the size of

the target cue in controlling immobilized cue concentration.

To highlight the controllability of immobilized cue concentration in this model, PR-Dex gels were

either irradiated for variable time lengths (Fig. 4A) or incorporated variable Acryl-PEG-CNBC(OMe)

concentrations (Fig. 4B) prior to introduction of MI-TR (729 Da). In Figure 4A, the concentration of

immobilized MI-TR in PR-Dex irradiated for 10 s was 7.60 ± 0.365 µM (n = 3) and 11.7 ± 0.161 µM for 30

s (n = 3). Gels irradiated for 60 s and 90 s bound MI-TR at concentrations of 16.9 ± 0.230 µM (n = 3) and

18.1 ± 0.452 µM (n = 3), respectively. All of these concentrations were statistically significant from each

other, thereby confirming irradiation time as a mechanism of controlling the concentration of the

presented cue. A similar trend in cue immobilization was observed in PR-Dex gels of varying Acryl-PEG-

CNBC(OMe) concentration. Gels with 2.02 mM of the photoreactive molecule bound MI-TR at a

concentration of 7.76 ± 0.0132 µM (n = 3), and gels with 4.04 mM of Acryl-PEG-CNBC(OMe) immobilized

11.8 ± 0.0882 µM MI-TR (n = 3). Bound MI-TR was present at concentrations of 13.1 ± 0.243 µM (n = 3)

and 18.1 ± 0.452 µM (n = 3) in PR-Dex gels with 6.06 mM and 8.08 mM Acryl-PEG-CNBC(OMe),

respectively. Thus, increasing the concentration of Acryl-PEG-CNBC(OMe) increases the concentration of

immobilized MI-TR. These results support the assumptions that both irradiation time and CNBC

concentration can be used to control the quantity of guidance cues present in PR-Dex.

3.2 Neurite growth in photoreactive dextran

The photoreactive dextran developed in this study provided an amenable scaffold for supporting

neurite growth in 3D. Neurites extending from DRG explants demonstrated robust growth in PR-Dex

after 5 days, as seen in Figure 5. Neurite growth (red) is restricted to the PR-Dex region by the PEG mold

boundary, and is of homogenous density across the primary channel. Glial cells (green) were contained

within the PEG boundary and mostly concentrated in the DRG explant, with some migration along the

neurites into the primary channel of PR-Dex. After 5 days, the glial cells had not yet migrated to the

channel bifurcation for any condition. From the images of Figure 5, it was observed that neurites tended

to first grow along the boundary between PEG and PR-Dex before navigating into the bulk of PR-Dex.

Because of this behavior, neurite growth was able to extend into both channels equally, despite the

difference in angle of the bifurcated channels compared to the primary PR-Dex channel. Confocal

imaging (Fig. 6) of neurites cultured in PR-Dex gels with immobilized NA confirmed that neurites

extended throughout the entire depth of the PR-Dex gel (213 µm), rather than a single plane. According

to the depth-coded image in Figure 6, most of the growth was concentrated to the center plane of the

gel between depths of about 40 µm to 125 µm, with height 0 µm being the cell culture membrane. This

finding was notable because it confirmed that the neurites were not growing strictly along the cell

culture membrane in 2D.

3.3 Neurite response to immobilized guidance cues

The response of neurites was quantified according to the previously stated guidance ratio, and

presented in Figure 7 (n = 7 for all conditions). Using this ratio, positive numbers indicate

chemoattraction, negative numbers indicate chemorepulsion, and zero indicates no response. Gels with

immobilized NA did not elicit an attractive or repulsive response, with a guidance ratio of 0.024 ± 0.043,

confirming NA as an appropriate control protein. Additionally, this supports the assumption that the

process of immobilizing proteins to PR-Dex does not in itself elicit a response from neurites.

For PR-Dex gels with the chemoattractive cue NT-3, a moderate attractive response was observed, with these gels having an overall guidance ratio of 0.18 ± 0.097. Conversely, gels with the chemorepulsive cue Sema3A elicited a strong repulsive response from neurites, with an average guidance ratio of -0.48 ± 0.16. These responses indicate that the neurites respond predictably to NT-3 and Sema3A when presented as immobilized cues. Statistical evaluation indicated that responses from both NT-3 and Sema3A were significant compared to the response to NA ($p < 0.005$), while a stronger difference in response was observed between NT-3 and Sema3A ($p < 0.001$). Neurites fully avoided the regions of bound Sema3A, as seen in Figure 5. This behavior confirms that unbound proteins were completely washed out from the dual hydrogel constructs, as the neurites grew robustly in regions without immobilized Sema3A. Neurites that grew in the Sema3A channel tended to extend along the boundary between the PEG mold and the PR-Dex channel, without fully crossing into the region of immobilized Sema3A. The neurite responses to both NT-3 and Sema3A indicate that neither the commercially available kit used to conjugate maleimide to the proteins nor the fluorescent secondary antibody affected the proteins' reactivity with cervical DRG neurites.

4. Discussion

The dual hydrogel constructs fabricated by the dynamic mask photolithography apparatus accommodated both structural and molecular control over 3D neurite outgrowth from DRGs in a simple and reproducible manner. One particularly useful aspect of this methodology was that the constructs could be fully assembled directly onto the cell culture insert membranes prior to the addition of live tissue. This meant that fabrication steps that would be otherwise harmful in the presence of neurites, such as chemically crosslinking PR-Dex with AP/TEMED, could still be performed, as any cytotoxic reagents are washed out prior to the addition of DRG explants. Additionally, multiple constructs could

be fabricated on each cell culture insert, promoting reproducibility, material conservation, and potentially high-throughput means for developing a 3D nerve growth assay.

The photoreactive dextran described in this study promoted robust growth of neurites and afforded a means to incorporate molecular cues without altering the integrity of the scaffold. The CNBC moiety of Acryl-PEG-CNBC provided a photocaged site for maleimide-conjugated biomolecules to bind. By using UV light to irradiate PR-Dex in selected regions, proteins could be incorporated into the scaffold in a spatially controlled manner, as UV light liberated the caging moiety of CNBC, thus exposing free thiols for maleimide-protein binding. Confocal imaging confirmed the homogenous immobilization of protein throughout the depth of PR-Dex, promoting equal exposure of proteins to the extending neurites. Because the biomolecules were covalently bound to the scaffold, the proteins remained in place for the duration of the experiment. This controlled spatial resolution was reinforced by the robust structural integrity of the dual hydrogel construct. Immobilizing cues of varying size to PR-Dex resulted in protein concentrations in a similar range, indicating that the concentration of free thiols, and thus CNBC moieties, was the governing factor for immobilized protein concentration. This is an easily exploitable benefit, as the concentration of Acryl-PEG-CNBC in the PR-Dex formula can be altered to change the final immobilized protein concentration. Additionally, because the dynamic photolithography apparatus irradiates substrates with a 3D extrusion of a 2D mask, the UV-light irradiation time may also be adjusted to affect the number of free thiols, thereby affecting the maximum possible concentration of maleimide-proteins. Thus, the photoreactive dextran presented in this study allows for two different methods for controlling the spatial distribution of immobilized proteins, promoting fine control over molecular guidance of cells in this model. The stiffness of PR-Dex may also be adjusted by altering the degree of methacrylation and the weight percent of dextran in the gel in order to accommodate different cell types.

To ensure that the process of immobilizing proteins in the PR-Dex gel did not affect neurite growth, the medium-weight protein NeutrAvidin (60.0 kDa) was chosen as the control, as NA does not elicit any response from neurites. The neurite outgrowth experiments performed in this study resulted in a non-specific response to NA by the neurites. Because neurites are sensitive to structural differences in their in vivo environment, an implicit guidance response would have been observed if the PR-Dex had undergone mechanical changes after UV irradiation or protein immobilization. Since the neurites did not exhibit any preference to either channel, this expected outcome to the control protein suggests that no significant structural changes occur in the PR-Dex gel during protein immobilization.

Both neurotrophin-3 and semaphorin 3A, with respective molecular weights of 13.6 kDa and 114 kDa, were conjugated with maleimide moieties using a commercially available kit without losing their reactivity. Though the relative bioactivity for either NT-3 or Sema3A after maleimide conjugation is not known, the proteins exhibited sufficient bioactivity to induce responses from the neurites. The response to the maleimide-conjugated cues supports the assumption that any protein with a free amine for maleimide conjugation can be immobilized to the PR-Dex scaffold, rendering the dual hydrogel construct non-specific to cell type for molecular guidance by immobilized cues.

Neurite growth from DRG explants extended throughout the depth of the PR-Dex gel and was contained within the PEG boundary. For our model to be an appropriate platform for investigating *in vivo* processes, it was essential to demonstrate the 3D nature of neurite growth in the dual hydrogel construct. Neurites primarily extended through the bulk of PR-Dex, without concentrating along the interface of the two gels, or along the cell culture membrane. Growth was robust through all planes of PR-Dex, indicating that dextran may be a useful polymer for developing nerve growth assays.

The incorporation of NT-3 and Sema3A in our model elicited predicable responses from DRG neurites. Cervical DRGs were used for this study due to their documented reactivity to NT-3 and Sema3A [10, 11, 15]. In the developing embryo, NT-3 accumulates at the limb buds to direct proprioceptive neurites

to their motor neuron targets [15]. While NT-3 is traditionally associated with the maintenance of sensory

neurons during nervous system mapping, recent studies have observed a chemoattractive response to

NT-3 in DRG neurites [9, 11]. Like most neurotrophins, NT-3 is a soluble factor that can become affinity-

immobilized in the extracellular matrix. In our model, we observed a moderate attractive response of

DRG neurites to a uniform presentation of covalently-immobilized NT-3. Since DRGs consist of both

proprioceptive and nociceptive fibers, it is expected that only a portion of neurites from the DRG explant

would possess TrkC receptors to bind NT-3 [8, 12]. Additionally, the response to NT-3 may be more

pronounced if NT-3 were presented as a gradient, as other *in vitro* studies have observed a graded

neurite response to changes in NT-3 concentration from 0 to 500 ng/ml (0 - 36.8 nM) [7, 11, 15, 16]. Because

our model is able to bind over four times the quantity of NT-3 used in other studies, establishing a

significant gradient of immobilized protein is very feasible, and has been previously demonstrated in an

earlier iteration of this model [28].

Neurites exhibited a strong repulsive response to immobilized Sema3A in our model. The

protein Sema3A induces growth cone collapse in DRG axons through actin cytoskeleton

depolymerization, and is presented as a transmembrane protein or a secreted guidance cue [1, 16, 34, 35].

Some *in vitro* studies have utilized the repulsive nature of Sema3A as an immobilized cue in

concentrations up to 50 nM, with DRG neurite responses to Sema3A increasing as protein concentration

increases [16, 20]. Here we have presented immobilized Sema3A in a substantial quantity and observed a

strong response by cervical DRG neurites, as seen in previous *in vitro* studies. Neurites extending

through all planes of PR-Dex navigated the boundary of the immobilized Sema3A region and redirected

toward the channel without Sema3A. This very distinct boundary between the neurite growth and the

immobilized cues indicated that the concentration of Sema3A was too high for neurites to overcome, as

neurites were unable to grow on the surface of the gel or the cell culture membrane in the Sema3A

region. Since the concentration of Sema3A present directly affects the neurite response to the protein,

neurites were observed to navigate the interface between PR-Dex and PEG where the concentration of Sema3A was assumed to be lower compared to the bulk PR-Dex since Sema3A did not bind to PEG. This behavior also indicates that any unbound and soluble protein is not accumulating at the interface between the two gels, thereby reaffirming that the protein is only present in the regions irradiated by UV light.

The ability to manipulate the structural and molecular presentation of guidance cues independently in this dual hydrogel system broadens the potential applications for cell growth assays. In our model, we observed 3D growth of neurites and elicited *in vivo* responses in an in vitro environment. Further investigation of the electrophysiological responses of the neurites growth in these substrates will help validate our model as an appropriate platform for neural cell culture assays. Future studies will expand the model for use with other neural cell types and guidance cues.

5. Conclusions

We have developed a 3D model for neurite growth using a novel photoreactive dextran gel and observed predictable responses to relevant immobilized guidance cues. The utility of the photolithography apparatus allowed for control over structural and molecular components of the dual hydrogel construct, as well as promoting reproducibility of results. The 3D model for neurite growth incorporated a choice point for cervical DRG neurites, and the immobilized chemoattractive and chemorepulsive cues elicited predictable and quantifiable responses. This model system can incorporate a wide range of maleimide-conjugated biomolecules, enhancing the utility of the system for use with a variety of cell types.

Acknowledgements

References

1.   M. Tessier-Lavigne and C. S. Goodman, *Science*, 1996, 274, 1123-1133.
2.   P. Lotfi, K. Garde, A. K. Chouhan, E. Bengali and M. I. Romero-Ortega, *Front Neuroeng*, 4, 11.
3.   J. Roy, T. E. Kennedy and S. Costantino, *Lab Chip*, 2013, 13, 498-508.
4.   L. Aloe, M. L. Rocco, P. Bianchi and L. Manni, *J Transl Med*, 2012, 10, 239.
5.   E. J. Huang and L. F. Reichardt, *Annu Rev Neurosci*, 2001, 24, 677-736.
6.   M. V. Chao, *Nat Rev Neurosci*, 2003, 4, 299-309.
7.   K. Moore, M. MacSween and M. Shoichet, *Tissue Eng*, 2006, 12, 267-278.
8.   X. Cao and M. S. Shoichet, *Neuroscience*, 2003, 122, 381-389.
9.   N. Usui, K. Watanabe, K. Ono, K. Tomita, N. Tamamaki, K. Ikenaka and H. Takebayashi, *Development*, 2012, 139, 1125-1132.
10. F. Hory-Lee, M. Russell, R. M. Lindsay and E. Frank, *Proc Natl Acad Sci U S A*, 1993, 90, 2613-2617.
11. B. Genc, P. H. Ozdinler, A. E. Mendoza and R. S. Erzurumlu, *PLoS Biol*, 2004, 2, e403.
12. D. A. Houweling, A. J. Lankhorst, W. H. Gispen, P. R. Bar and E. A. J. Joosten, *Experimental Neurology*, 1998, 153, 49-59.
13. L. Taylor, L. Jones, M. H. Tuszynski and A. Blesch, *Journal of Neuroscience*, 2006, 26, 9713-9721.
14. S. Beggs, D. Alvares, A. Moss, G. Currie, J. Middleton, M. W. Salter and M. Fitzgerald, *Pain*, 2012, 153, 2133-2139.
15. T. Ringstedt, J. Kucera, U. Lendahl, P. Ernfors and C. F. Ibanez, *Development*, 1997, 124, 2603-2613.
16. E. K. Messersmith, E. D. Leonardo, C. J. Shatz, M. Tessierlavigne, C. S. Goodman and A. L. Kolodkin, *Neuron*, 1995, 14, 949-959.
17. B. Rohm, A. Ottemeyer, M. Lohrum and A. W. Puschel, *Mechanisms of Development*, 2000, 93, 95-104.
18. F. Polleux, T. Morrow and A. Ghosh, *Nature*, 2000, 404, 567-573.
19. W. J. Rosoff, J. S. Urbach, M. A. Esrick, R. G. McAllister, L. J. Richards and G. J. Goodhill, *Nature Neuroscience*, 2004, 7, 678-682.
20. B. Joddar, A. T. Guy, H. Kamiguchi and Y. Ito, *Biomaterials*, 2013, 34, 9593-9601.
21. R. J. Pasterkamp, R. J. Giger, M. J. Ruitenberg, A. J. G. D. Holtmaat, J. De Wit, F. De Winter and J. Verhaagen, *Molecular and Cellular Neuroscience*, 1999, 13, 143-166.
22. R. J. Pasterkamp, P. N. Anderson and J. Verhaagen, *European Journal of Neuroscience*, 2001, 13, 457-471.
23. S. Kaneko, A. Iwanami, M. Nakamura, A. Kishino, K. Kikuchi, S. Shibata, H. J. Okano, T. Ikegami, A. Moriya, O. Konishi, C. Nakayama, K. Kumagai, T. Kimura, Y. Sato, Y. Goshima, M. Taniguchi, M. Ito, Z. G. He, Y. Toyama and H. Okano, *Nature Medicine*, 2006, 12, 1380-1389.
24. C. A. DeForest and K. S. Anseth, *Angew Chem Int Ed Engl*, 51, 1816-1819.
25. K. A. Mosiewicz, L. Kolb, A. J. van der Vlies, M. M. Martino, P. S. Lienemann, J. A. Hubbell, M. Ehrbar and M. P. Lutolf, *Nat Mater*, 12, 1072-1078.
26. R. G. Wylie, S. Ahsan, Y. Aizawa, K. L. Maxwell, C. M. Morshead and M. S. Shoichet, *Nat Mater*, 10, 799-806.
27. Y. Luo and M. S. Shoichet, *Biomacromolecules*, 2004, 5, 2315-2323.
28. E. L. Horn-Ranney, J. L. Curley, G. C. Catig, R. M. Huval and M. J. Moore, *Biomedical Microdevices*, 2013, 15, 49-61.
29. Y. Luo and M. S. Shoichet, *Nature Materials*, 2004, 3, 249-253.
30. J. L. Curley and M. J. Moore, *Journal of Biomedical Materials Research Part A*, 2011, 99A, 532-543.

31.   S. Z. Zhou, A. Bismarck and J. H. G. Steinke, *Journal of Materials Chemistry*, 2012, 22, 18824-18829.

32.   X. W. Li, E. Katsanevakis, X. Y. Liu, N. Zhang and X. J. Wen, *Progress in Polymer Science*, 2012, 37, 1105-1129.

33.   K. Shroff, E. L. Rexeisen, M. A. Arunagirinathan and E. Kokkoli, *Soft Matter*, 2010, 6, 5064-5072.

34.   H. Aizawa, S. Wakatsuki, A. Ishii, K. Moriyama, Y. Sasaki, K. Ohashi, Y. Sekine-Aizawa, A. Sehara-Fujisawa, K. Mizuno, Y. Goshima and I. Yahara, *Nature Neuroscience*, 2001, 4, 367-373.

35.   C. X. Li, Y. Sasaki, K. Takei, H. Yamamoto, M. Shouji, Y. Sugiyama, T. Kawakami, F. Nakamura, T. Yagi, T. Ohshima and Y. Goshima, *Journal of Neuroscience*, 2004, 24, 6161-6170.

Figures
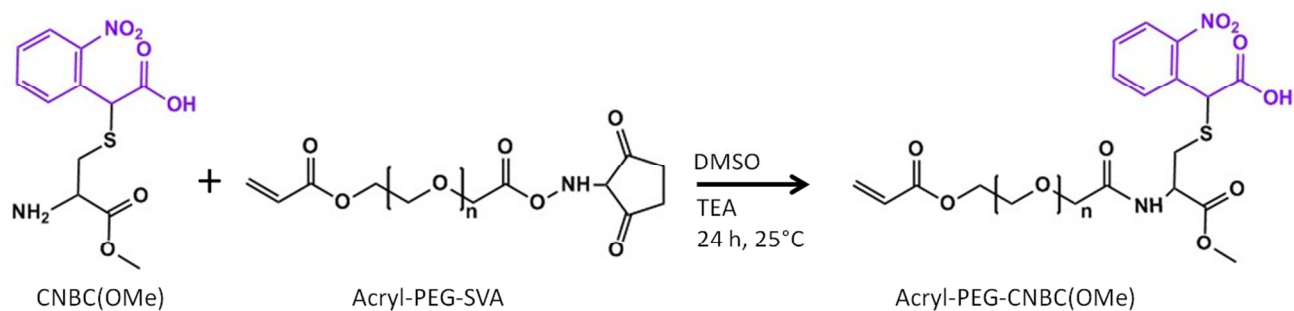
Figure 1. Synthesis of Acryl-PEG-CNBC(OMe). S-(α-carboxy-2-nitrobenzyl)-L-cysteine methyl ester (CNBC(OMe)) is mixed with Acryl-Polyethylene Glycol-Succinimidyl valerate (Acryl-PEG-SVA) in DMSO. Triethylamine (TEA) is added to the solution, and the reaction is carried out for 24 at room temperature to yield Acryl-PEG-CNBC(OMe). The carboxy-nitrobenzyl moiety (purple) is UV-light sensitive.
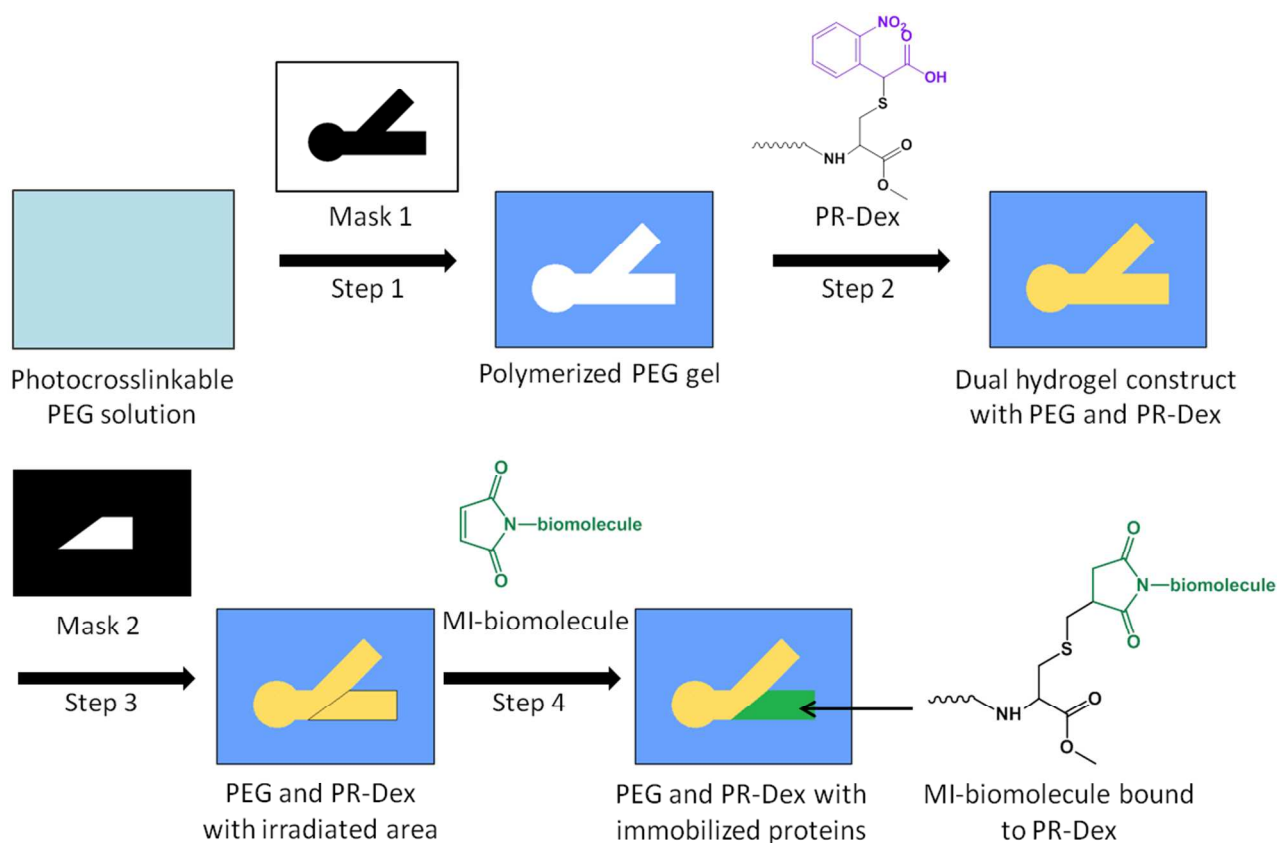
Figure 2. Fabrication scheme for dual hydrogel constructs with photoreactive dextran (PR-Dex) and immobilized cues. Step 1: A cell culture insert is filled with photocrosslinkable PEG solution. Using Mask 1, PEG solution is crosslinked via UV irradiation and uncrosslinked PEG is removed. Step 2: The PEG molds are filled with PR-Dex solution and chemically crosslinked via APS/TEMED. The photocleavable moiety on PR-Dex (purple) cages the thiol on the cysteine. Step 3: After gelation, PR-Dex is irradiated with UV using Mask 2. Irradiation uncages the thiol moiety on PR-Dex, providing a binding site for maleimide-activated (MI) biomolecules. Step 4: Inserts are soaked in MI-biomolecule solution tagged with fluorescent markers, resulting in a region of immobilized MI-biomolecules in PR-Dex.
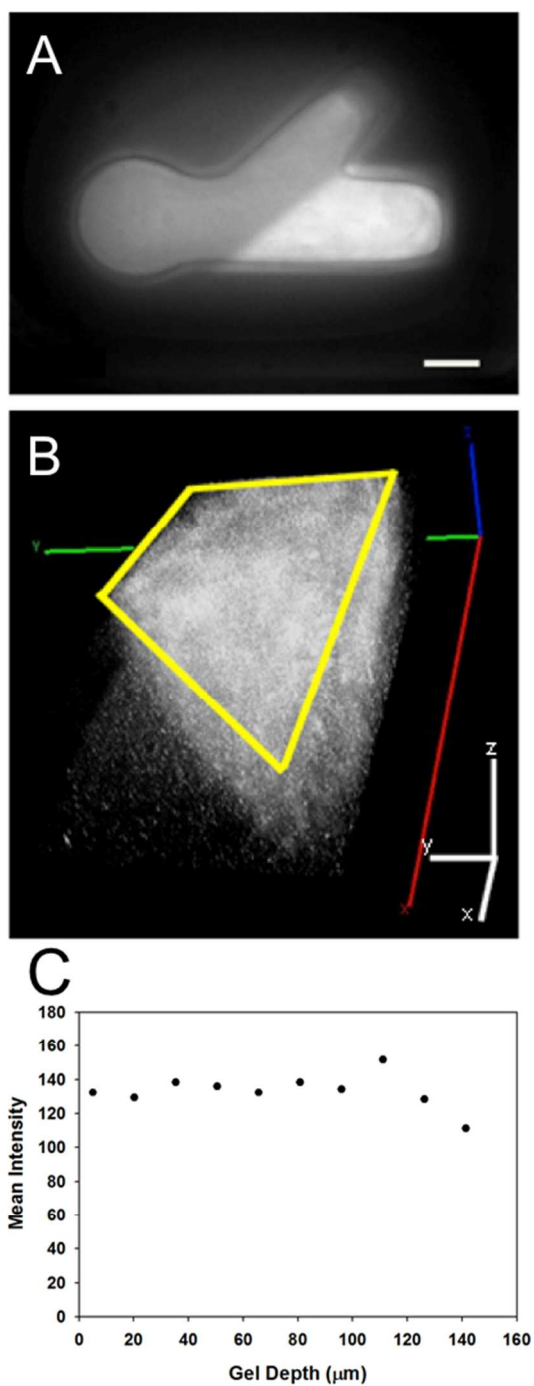
Figure 3. Immobilized proteins in PR-Dex. (A) NeutrAvidin (NA) tagged with AF488 biocytin immobilized in UV-irradiated PR-Dex (scale bar = 1 mm). (B) 3D confocal reconstruction of NA immobilized through the depth of PR-Dex (227 μm); yellow outline indicates trapezoidal NA region seen in top image (scale = 200 μm). (C) Graph of average fluorescence intensity (arbitrary units) throughout depth of immobilized region, indicating relative uniform protein distribution throughout depth of gel.

Table 1. Quantification of immobilized proteins in PR-Dex. Concentration is presented as mean ± standard deviation (n = 4-6).

| Protein	Molecular Weight (kDa)	Concentration (nM)
NeutrAvidin	60.0	122 ± 2.50
Neurotrophin-3	13.6	151 ± 15.7
Semaphorin 3A	114	87.6 ± 6.74
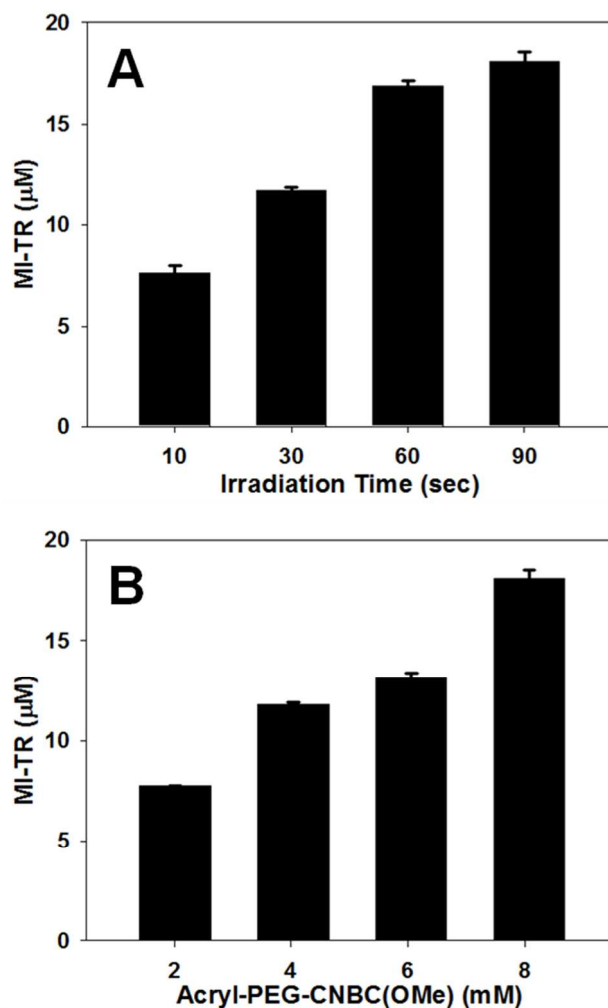
Figure 4. Graphs of immobilized maleimide-conjugated Texas Red (MI-TR) in PR-Dex. Solid bars represent mean concentration of immobilized MI-TR in PR-Dex gels with either (A) variable UV irradiation times, or (B) variable concentrations of Acryl-PEG-CNBC(OMe). All means are statistically significant from each other (A: $p < 0.05$; B: p , 0.005). Error bars represent standard deviation (n = 3).
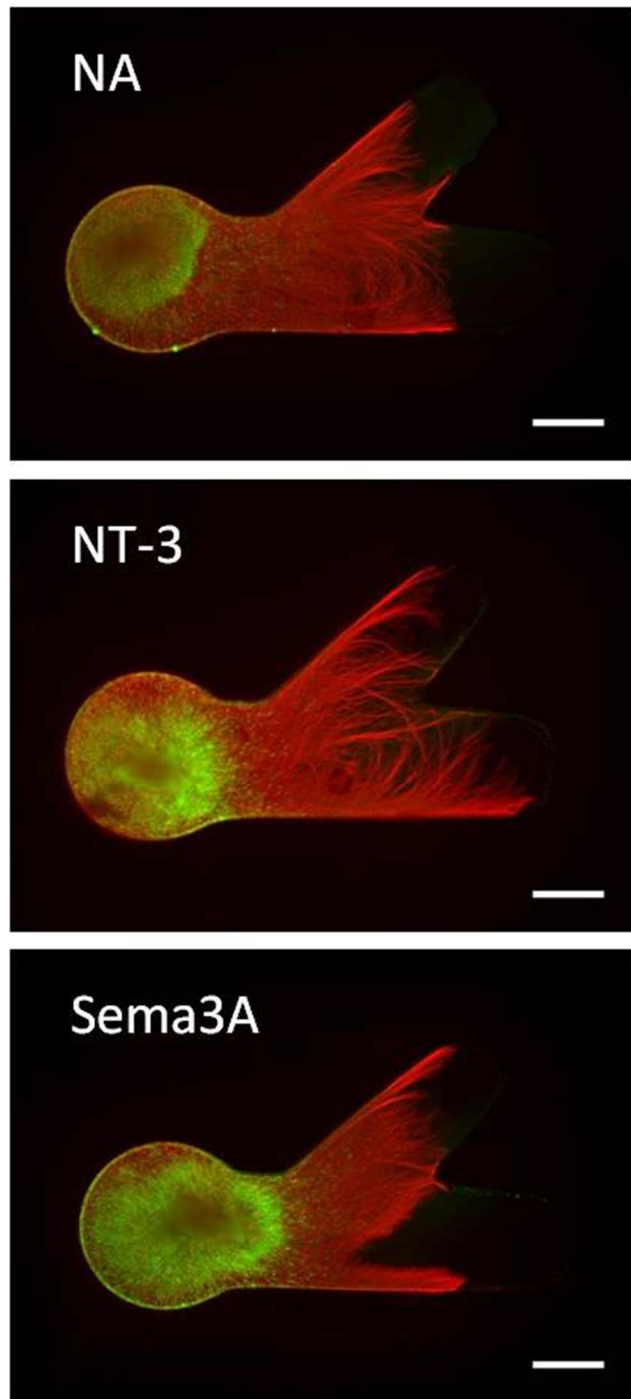
Figure 5. Neurite growth in the presence of immobilized cues. Dorsal root ganglia are cultured in the presence of immobilized NeutrAvidin (NA), neurotrophin-3 (NT-3) and semaphorin 3A (Sema3A). Neurites are stained with βIII tubulin (red) and glial cells are stained with S100 (green). Scale bars = 500 µm.
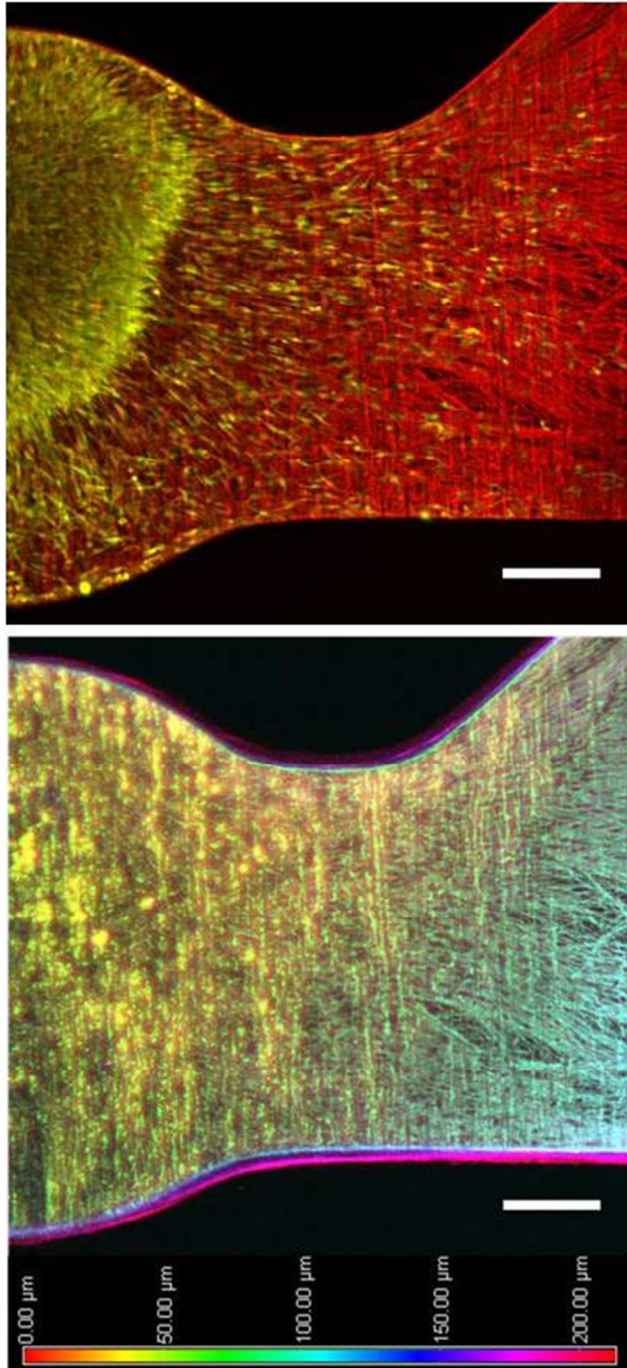
Figure 6. Confocal image of neurite growth in dual hydrogel constructs. Top) Z-projection of neurites (red) and glial cells (green) in PR-Dex with immobilized NA. Bottom) Depth-coded image of neurites extending 213 μm through depth of PR-Dex. Scale bars = 200 μm.
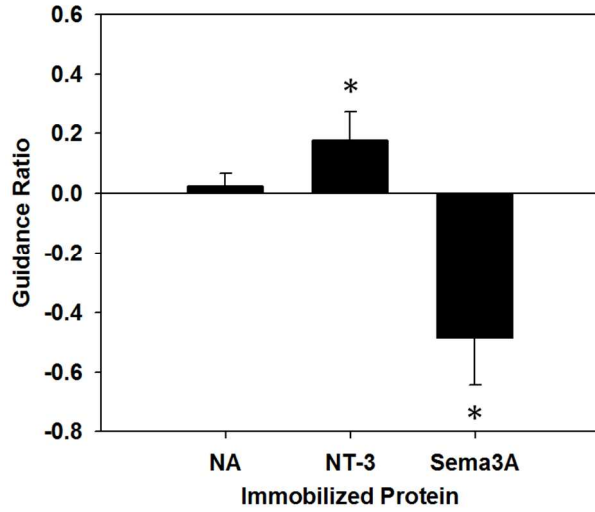
Figure 7. Graph of neurite guidance ratios. Positive values indicate an attractive response, while negative values indicate a repulsive response. The neurite response to either neurotrophin-3 (NT-3) or semaphorin 3A (Sema3A) was statistically significant from responses to NeutrAvidin (NA) at a confidence level of $p < 0.005$. Error bars represent standard deviation (n = 7).

Graphical Abstract
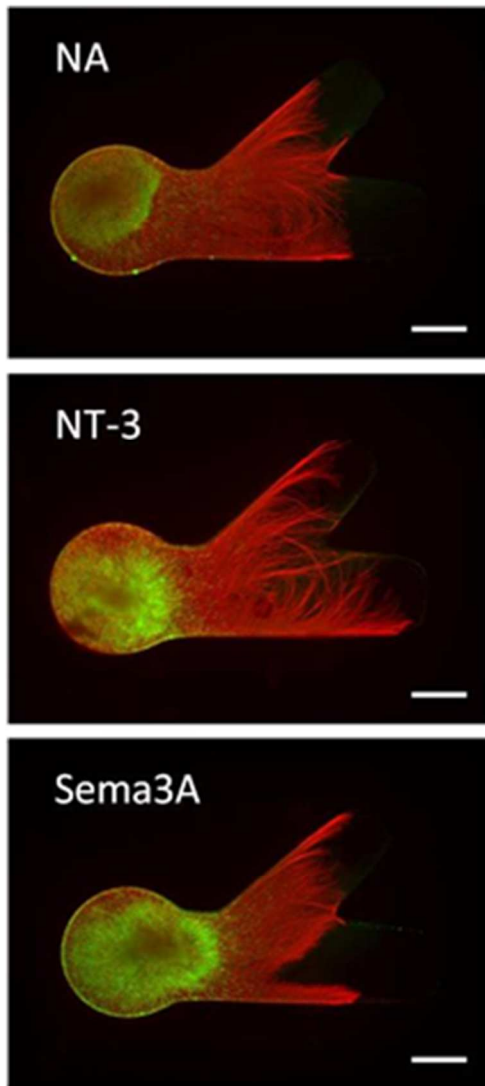
Immobilized NT-3 enhanced DRG neurite growth while Sema3A strongly repelled it, versus neutravidin controls, in a hydrogel choice point model.